

Targeting the hepatitis B virus precore antigen with a novel IgNAR single variable domain intrabody

Renae Walsh^{a,*}, Stewart Nuttall^b, Peter Revall^a, Danni Colledge^a, Liza Cabuang^{a,1}, Sally Soppe^a, Olan Dolezal^b, Kate Griffiths^{b,2}, Angeline Bartholomeusz^{a,3}, Stephen Locarnini^a

^a Victorian Infectious Diseases Reference Laboratories, 10 Wreckyn Street, North Melbourne, Victoria 3051, Australia

^b CSIRO Molecular and Health Technologies, 343 Royal Parade, Parkville, Victoria 3052, Australia

ARTICLE INFO

Article history:

Received 28 September 2010
Returned to author for revision
27 October 2010
Accepted 20 December 2010
Available online xxxx

Keywords:

Hepatitis B e antigen
Precore
Chronic hepatitis B
New antigen receptor
Intrabody
Endoplasmic reticulum
BLAcore kinetics
Bacteriophage display

ABSTRACT

The Hepatitis B virus precore protein is processed in the endoplasmic reticulum (ER) into secreted hepatitis B e antigen (HBeAg), which acts as an immune tolerogen to establish chronic infection. Downregulation of secreted HBeAg should improve clinical outcome, as patients who effectively respond to current treatments (IFN- α) have significantly lower serum HBeAg levels. Here, we describe a novel reagent, a single variable domain (V_{NAR}) of the shark immunoglobulin new antigen receptor (IgNAR) antibodies. V_{NARS} possess advantages in stability, size (~14 kDa) and cryptic epitope recognition compared to conventional antibodies. The V_{NAR} domain displayed biologically useful affinity for recombinant and native HBeAg, and recognised a unique conformational epitope. To assess therapeutic potential in targeting intracellular precore protein to reduce secreted HBeAg, the V_{NAR} was engineered for ER-targeted *in vitro* delivery to function as an intracellular antibody (intrabody). *In vitro* data from HBV/precore hepatocyte cell lines demonstrated effective intrabody regulation of precore/HBeAg.

© 2010 Elsevier Inc. All rights reserved.

Introduction

Hepatitis B virus (HBV) affects more than 350 million people globally and is a major health concern causing acute and chronic liver disease, leading to hepatocellular carcinoma and cirrhosis (Kane, 1996; Lavanchy, 2004). Chronic hepatitis B (CHB) is the 10th leading cause of death worldwide (Lavanchy, 2004). The precore or hepatitis B e antigen (HBeAg) and core or HBeAg are encoded by the precore (preC-C) gene, and are transcribed from separate, although highly homologous, RNA transcripts. Accordingly, the two proteins share significant amino acid identity (Fig. 1), although likely structural differences between these proteins, due to the 10 unique residues at the HBeAg N-terminus, may also mediate antigenic variation (Revill et al., 2010). The mature intracellular HBeAg protein (p21) of 183 residues (~21 kDa) includes an arginine-rich DNA binding protamine domain at the C-terminus, and forms the viral nucleocapsid. The

precore precursor protein (p25) is processed into the HBeAg as follows. A 29-residue signal peptide at the N-terminus directs the precursor protein to the endoplasmic reticulum for two-step processing. Initially, the 19 N-terminal residues are cleaved (Dienes et al., 1995) to produce an intracellular intermediate (p22). Next, the 34 residues encoding the arginine-rich protamine domain are cleaved from the C-terminus by a furin-like protease (Messageot et al., 2003; Takahashi et al., 1983) to produce the HBeAg protein (p17), which is a secreted protein of 159 residues (~17 kDa) (Milich et al., 1998). Functionally, the role of HBeAg in the viral life cycle is poorly understood (Chen et al., 2003). The HBeAg is a secreted accessory protein, which appears to attenuate the host immune response to the intracellular nucleocapsid protein (Chang et al., 1987; Chen et al., 2004). The HBeAg acts as an immune tolerogen contributing to HBV persistence (Chen et al., 2005), and possibly functions *in utero* considering that soluble HBeAg traverses the placenta (Milich et al., 1990). Furthermore, HBeAg downregulates: i) cellular genes controlling intracellular signaling (Locarnini et al., 2005); and ii) the Toll-like receptor 2 (TLR-2) to dampen the innate immune response to viral infection (Riordan et al., 2006; Visvanathan et al., 2007). In the absence of HBeAg, HBV replication is associated with upregulation of the TLR2 pathway (Visvanathan et al., 2007). Taken together, the reported data suggest that HBeAg has a significant role in modulating virus/host interactions to influence the host immune response.

* Corresponding author. Fax: +61 3 9342 2666.

E-mail address: renae.walsh@mh.org.au (R. Walsh).

¹ Present Address: National Serology Reference Laboratory, 41 Victoria Parade, Fitzroy, Victoria 3065, Australia.

² Present Address: AdAlta Pty Ltd, Park Drive, Bundoora, Victoria 3083, Australia.

³ Present Address: Murdoch Childrens Research Institute, Flemington Road, Parkville, Victoria 3052, Australia.

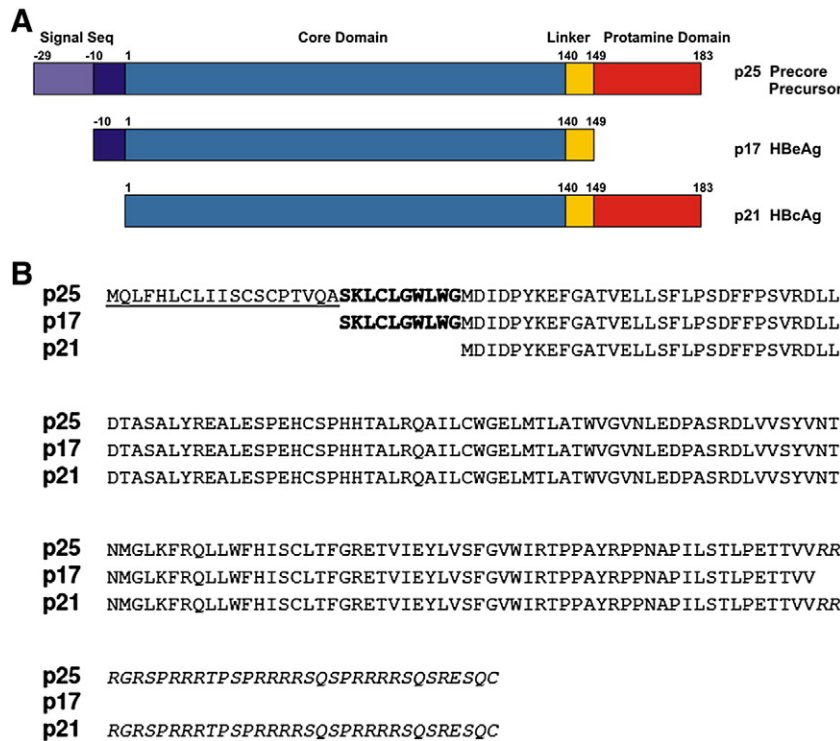


Fig. 1. Processing and comparative alignment of HBeAg and HBcAg (genotype D). (A) the precore precursor protein (p25) is processed N- and C-terminally to produce the HBeAg (p17) of 159 residues (~18 kDa), numbered –10 to 149. The 10 N-terminal signal sequence residues are unique to HBeAg. The HBcAg (p21), produced from a separate RNA transcript, consists of 183 residues (~21 kDa) numbered 1–183, and has 34 unique residues at the C-terminus. The HBeAg and HBcAg share a common core domain of 149 residues. (B) sequence alignment of p25, p17 and p21 proteins, highlighting the 10 N-terminal unique residues of p17 (bold), the 19mer N-terminal ER signal sequence of p25 precursor (underlined), and the 34 C-terminal residues specific for p21 (italicised).

Therefore, intracellular regulation of precore protein and HBeAg secretion could exert a potential antiviral effect, and may be of future clinical relevance.

The immunoglobulin new antigen receptor (IgNAR) is a unique antibody isotype found in cartilaginous fish (sharks and possibly rays), and both immune and naïve molecular libraries of IgNAR variable domains have been constructed and screened to isolate binding reagents (Greenberg et al., 1995; Nuttall et al., 2001). IgNARs are bivalent, but target antigen through a single immunoglobulin variable domain (~14 kDa) displaying two complementarity determining region (CDR) loops attached to varying numbers of constant domains (Nuttall et al., 2003; Roux et al., 1998). In contrast, traditional immunoglobulin (Ig) antibodies have a variable heavy (V_H) + variable light (V_L) domain format (~26 kDa) and bind antigen through up to six CDRs (Chothia et al., 1989; Padlan, 1994). The small size and thermodynamic and chemical stability (Nuttall et al., 2004) of IgNAR variable domains (V_{NAR} s) offer distinct advantages over conventional antibodies. Furthermore, V_{NAR} domains access cryptic antigenic epitopes through unusually long and variable CDR3 loops (Nuttall et al., 2004; Stanfield et al., 2004; Streltsov et al., 2004, 2005). These novel V_{NAR} qualities make them an attractive immunoglobulin scaffold to be developed for targeted intracellular antibody (intrabody) delivery *in vitro*, and subsequent development as an *in vivo* immunoglobulin therapy. Intrabodies utilising alternative scaffolds have previously been reported targeting several other viral proteins (reviewed in Nuttall and Walsh, 2008), including the HBV surface and core antigens (Serruys et al., 2009, 2010).

Here, we describe the isolation, characterisation and development of a V_{NAR} domain targeting HBeAg as an anti-HBe intrabody. We analyse specificity, binding kinetics, and epitope recognition to demonstrate the V_{NAR} utility in target antigen recognition. Furthermore, we assess future therapeutic potential of the anti-HBe V_{NAR} through investigation of the *in vitro* effects on intracellular and

extracellular precore/HBeAg regulation, following development of the V_{NAR} as an endoplasmic reticulum (ER) localised intrabody.

Results

Isolation and characterisation of HBV HBeAg/HBcAg specific V_{NAR}

To identify novel single-domain binding reagents against recombinant HBeAg target antigen, we screened a naïve V_{NAR} display bacteriophage library (Nuttall et al., 2003). Variability focused on the long V_{NAR} CDR3 loop (15–18 residues), and to a lesser extent within the CDR1 and framework regions (Nuttall et al., 2003). An increase in eluted bacteriophage titre (~100-fold) was observed between biopanning rounds 3 and 4 (data not shown), with 100% of colonies positive for V_{NAR} sequences by colony PCR (data not shown), indicating positive selection. ELISA analysis of the isolated V_{NAR} s using HBeAg identified a group of similar clones that showed marked binding above background, and upon further analysis, all could be classified into one of two sequence types, differing at only 4 residues. Of these, the clones designated H6 and H3, represent the two identified sequence types. The deduced amino acid sequences of V_{NAR} clones H6 and H3 are presented in Fig. 2A, and further incorporate in-frame dual octapeptide FLAG epitope tags and two alanine linker regions at the C-terminus. These sequences revealed typical V_{NAR} domains of 113 residues, with large (18 residue) CDR3 loops and an invariant disulphide bridge (Cys²²–Cys⁸³) connecting the two β -sheets, typical of the immunoglobulin fold (illustrated in Fig. 2B). Two further cysteine residues present within the CDR1 and CDR3 loop regions (Cys²⁹ and Cys⁹⁵) are consistent with formation of an interloop disulphide bridge (Streltsov et al., 2005). Dominant selection of just two clones after four rounds of biopanning represents a high enrichment factor (>10⁸). Such positive selection may be due to high affinity for the target antigen, and/or by a competitive advantage provided by superior expression qualities of

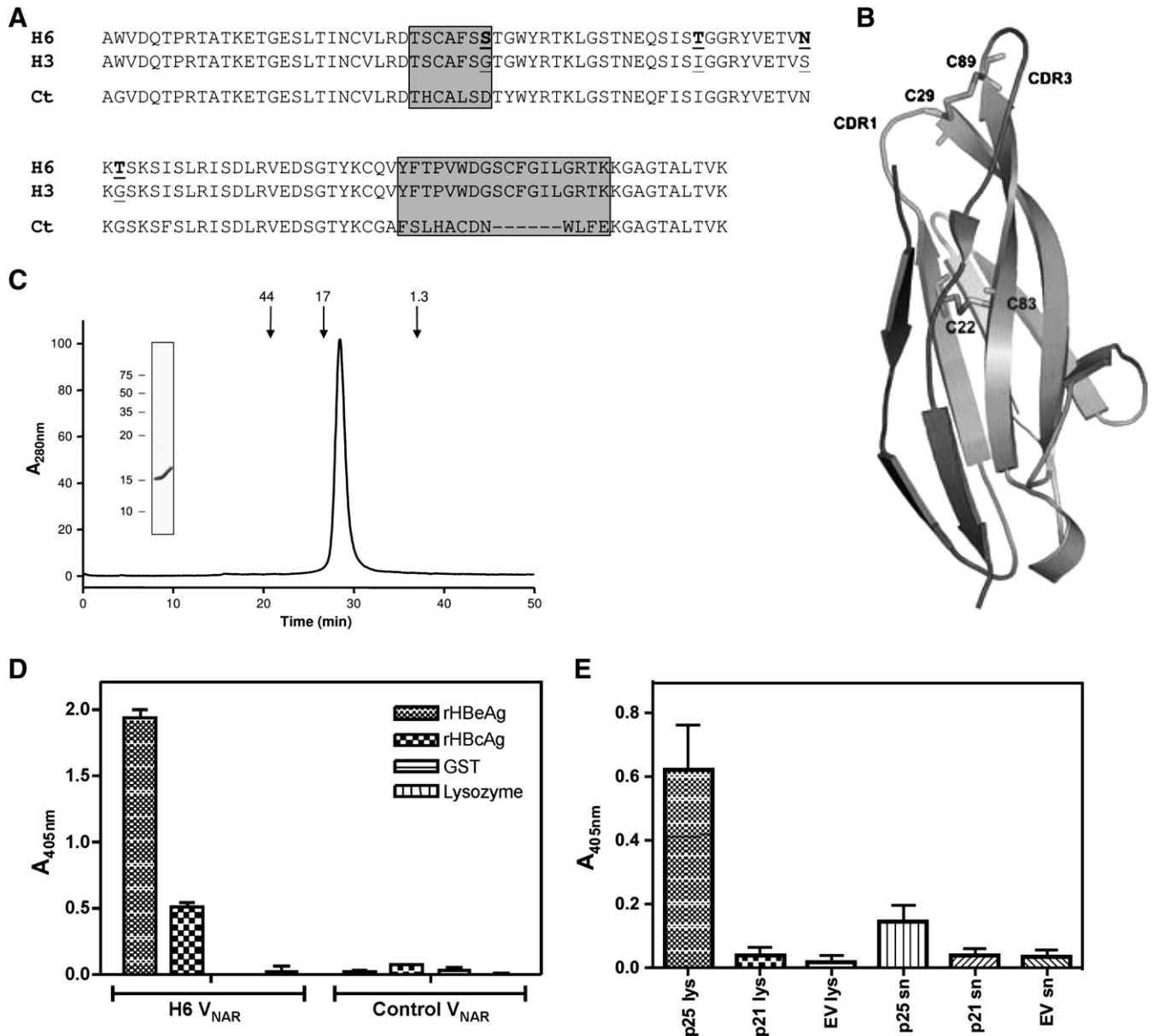


Fig. 2. Identification of HBeAg/HBcAg specific V_{NAR} s. (A) alignment of the amino acid sequences of the two isolated V_{NAR} s, H6 and H3 (Accession numbers EU213060 and EU213061). The four dissimilar residues are indicated in bold and underlined. The CDR1 and CDR3 regions are boxed and shaded for identification. Also included is the non-specific library clone control V_{NAR} (Ct) sequence. (B) A 'typical' V_{NAR} , in this case the 12A-9 clone (PDB: 2COQ [47]), illustrating the canonical (22–83) and inter-CDR (CDR1–CDR3; 29–89) disulphide bridges. Note the absence of a CDR2 loop region. (C) SEC elution profile of affinity-purified H6 V_{NAR} protein. The peak eluting at 29 min is consistent with a monomeric domain (theoretical molecular mass 14.7 kDa). The absorbance at $A_{280\text{nm}}$ is given in arbitrary units. Standard molecular masses in kDa are indicated. The inset in shows the V_{NAR} H6 sample analysed by SDS-PAGE (10%). (D) Comparative ELISA analysis of the binding specificity of V_{NAR} H6 with non-specific control V_{NAR} domain for immobilised HBeAg and HBcAg purified target antigens, and for GST and lysozyme (negative control proteins). Data represent the average of triplicate wells and are normalised to PBS background. (E) Analysis of V_{NAR} H6 affinity by ELISA for *in vitro* expressed HBeAg/HBcAg. Purified H6 V_{NAR} coated to ELISA plate wells was tested for binding affinity to p25 (HBeAg) and p21 (HBcAg) produced in transiently transfected Huh-7 cells, localised to the cell lysate (lys) or exported into culture supernatant (sn). Empty vector (EV) was incorporated as a control. Data represent the average of quadruplicate wells from duplicate experiments.

the selected proteins. Interestingly, the sequence of residues at the framework CDR3 junction (residues 83–85), suggest that this family is derived from the native shark repertoire (Dooley and Flajnik, 2006). Expressed and purified V_{NAR} eluted as single peak by size exclusion chromatography (SEC) (Fig. 2C), corresponding to a protein of ~14.7 kDa, consistent with the expected size of a monomeric V_{NAR} domain (Fig. 2C). The H6 and H3 protein expression characteristics and size exclusion chromatography profiles were almost identical, emphasising the similarity of the two proteins.

Based on superior target antigen recognition and the anti-HBe specificity of V_{NAR} H6 demonstrated by ELISA (Fig. 2D), the H6 V_{NAR} was selected for further study. The H6 V_{NAR} recombinant protein

displayed strong recognition for HBeAg ($A_{405\text{nm}}$ 1.94 ± 0.1), and exhibited weak cross-reaction for truncated HBcAg ($A_{405\text{nm}}$ 0.52 ± 0.04) (Fig. 2D), both of which are a mix of dimer and capsid protein format by SEC (data not shown). This indicates that the V_{NAR} binding site lies within the 149 residues that are common to both HBeAg and HBcAg (Fig. 1), but that the HBeAg is dominantly recognised, likely due to slight variations in the structural conformation of HBeAg compared with HBcAg (truncated) mediated by the unique N-terminal 10 residues (Reville et al., 2010). Non-specific affinity was not observed to the control antigens (GST or lysozyme). Furthermore, non-specific V_{NAR} binding to HBeAg or HBcAg was not apparent as a control V_{NAR} domain (a non-specific library clone, Fig. 2A, Ct) failed to display any

response for HBeAg or HBcAg ($A_{405\text{nm}}$ 0.03 ± 0.01 and 0.07 ± 0.01 respectively, Fig. 2D). The H6 V_{NAR} displayed reactivity to precore (p25) antigen expressed in Huh7 lysates (Fig. 2E), although reactivity to *in vitro* produced core (p21) protein was not apparent, suggesting H6 V_{NAR} is specific for *in vitro* precore protein.

V_{NAR} binding affinity analysis

To determine the H6 V_{NAR} binding kinetics, HBeAg or HBcAg GST-tag fusion proteins were captured to an α -GST surface for surface Plasmon resonance (SPR) measurements using a Biacore T100 (Fig. 3A). This configuration correctly orientated the HBeAg and HBcAg on the chip for measuring (in triplicate) the binding interactions with the V_{NAR} domain analytes. Consistent with the ELISA findings, the H6 (and H3) V_{NAR} displayed binding recognition for (SEC purified) recombinant HBeAg and HBcAg target proteins (Figs. 3B, C), and furthermore the H6 V_{NAR} target antigen binding was again superior to the H3 clone (Table 1). There was no binding of the H6 monomer to a blank surface (data not shown). The binding

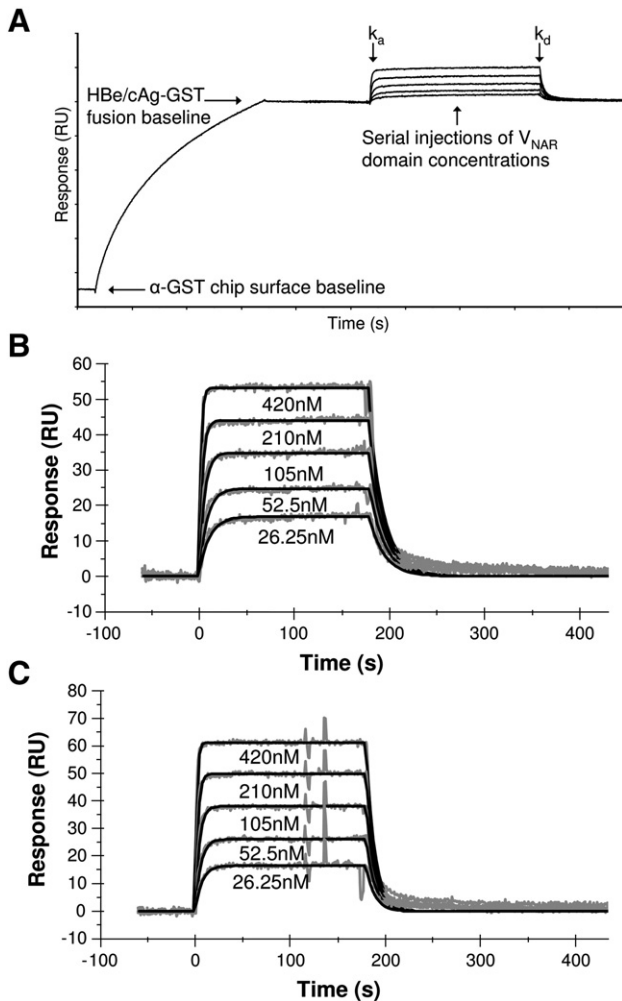


Fig. 3. Binding interactions of H6 V_{NAR} with HBeAg and HBcAg target antigens. (A) overview of Biacore SPR experiments, illustrating α -GST and HB(e/c)Ag-GST binding surface baselines for analysis of V_{NAR} binding kinetics. (B–C) overlaid Biacore sensorgrams showing the interaction between HBeAg or HBcAg, and peak-purified monomeric H6 V_{NAR} (ranging from 26.25 to 420 nM) analyte. The HBeAg-GST or HBcAg-GST fusion protein was captured by binding to an immobilised mouse anti-GST antibody; V_{NAR} analyte binding was measured in HBS buffer at a constant flow rate of $30 \mu\text{l}/\text{min}$ with an injection volume of $90 \mu\text{l}$. Data were averaged from triplicate experiments (B) Binding affinity interactions of captured HBeAg-GST with V_{NAR} H6 analyte; (C) Binding affinity interactions of captured HBcAg-GST with V_{NAR} H6 analyte.

Table 1
Binding affinities of V_{NAR} H6 and H3 for HBeAg and HBcAg target proteins.

Target Ag	V_{NAR}	k_a ($\text{M}^{-1} \text{s}^{-1}$)	k_d (s^{-1})	Kinetic K_D (nM)	Equilibrium K_D (nM)	Overall K_D (nM)
HBeAg	H6	$1.3 \pm 0.2 \times 10^6$	$6.1 \pm 0.3 \times 10^{-2}$	49 ± 3.8	57	53 ± 5.7
	H3	$8.6 \pm 0.9 \times 10^5$	$8.8 \pm 1.7 \times 10^{-2}$	101	110	106 ± 6.6
HBcAg	H6	$1.5 \pm 0.2 \times 10^6$	$10.8 \pm 0.6 \times 10^{-2}$	74	105	90 ± 22
	H3	$1.0 \pm 0.9 \times 10^5$	$14.0 \pm 1.1 \times 10^{-2}$	140	152	146 ± 8.7

reaction pattern indicated rapid association of V_{NAR} H6 with HBeAg and HBcAg to reach reaction equilibrium, which was followed by rapid dissociation (Figs. 3B, C). The rapid realisation of reaction equilibrium allowed for determination of binding parameters using both kinetic and equilibrium analysis methods. The various binding affinities and reaction rates are summarised in Table 1. Significant observations include: (i) the highest affinity (53 nM) was between H6 and HBeAg (Fig. 3B); and (ii) the affinity (90 nM) between H6 and HBcAg (truncated) was 1.7-fold weaker (Fig. 3C). The H6 binding data consistently indicated an increased affinity for HBeAg compared to HBcAg (truncated); therefore we hypothesise that the binding epitope is better displayed by HBeAg due to minor structural variations in protein folding influenced by the 10 unique residues at the N-terminus (Revill et al., 2010). Determination of the epitope binding site may ultimately require the co-crystallisation resolution of the HBeAg-H6 V_{NAR} and/or HBcAg-H6 V_{NAR} binding complexes, which could also facilitate further maturation of the H6 V_{NAR} to improve HBeAg affinity and specificity, through targeted structural manipulation of the CDR3 loop residues.

Immunoassay epitope mapping of V_{NAR} H6

We hypothesised that the H6 V_{NAR} recognises a conformational epitope, based on previous IgNAR publications that suggest the extended V_{NAR} CDR3 loop enables access to cryptic antigen pockets (Nuttall et al., 2004; Stanfield et al., 2004; Streltsov et al., 2004, 2005). Binding recognition of H6 V_{NAR} to HBeAg was not affected in competitive ELISA binding with several conventional anti-HBe/HBc antibodies (data not shown), which suggested the H6 V_{NAR} recognizes an alternative and non-proximally obscured HBeAg epitope to the tested anti10 HBe/c antibodies. Peptide library mapping of the H6 V_{NAR} using overlapping linear HBeAg epitopes (residues -10 to 149) further confirmed that the H6 V_{NAR} recognises a conformational epitope (data not shown). The H6 V_{NAR} displayed no specific recognition for any of the HBeAg peptides, and neither did the control V_{NAR} , although a strong binding response was elicited to full-length recombinant HBeAg.

Immunoassay epitope mapping of V_{NAR} H6

We hypothesised that the H6 V_{NAR} recognises a conformational epitope, based on previous IgNAR publications that suggest the extended V_{NAR} CDR3 loop enables access to cryptic antigen pockets (Nuttall et al., 2004; Stanfield et al., 2004; Streltsov et al., 2004, 2005). Binding recognition of H6 V_{NAR} to HBeAg was not affected in competitive ELISA binding with several conventional anti-HBe/HBc antibodies (data not shown), which suggested the H6 V_{NAR} recognizes an alternative and non-proximally obscured HBeAg epitope to the tested anti10 HBe/c antibodies. Peptide library mapping of the H6 V_{NAR} using overlapping linear HBeAg epitopes (residues -10 to 149) further confirmed that the H6 V_{NAR} recognises a conformational epitope (data not shown). The H6 V_{NAR} displayed no specific recognition for any of the HBeAg peptides, and neither did the control V_{NAR} , although a strong binding response was elicited to full-length recombinant HBeAg.

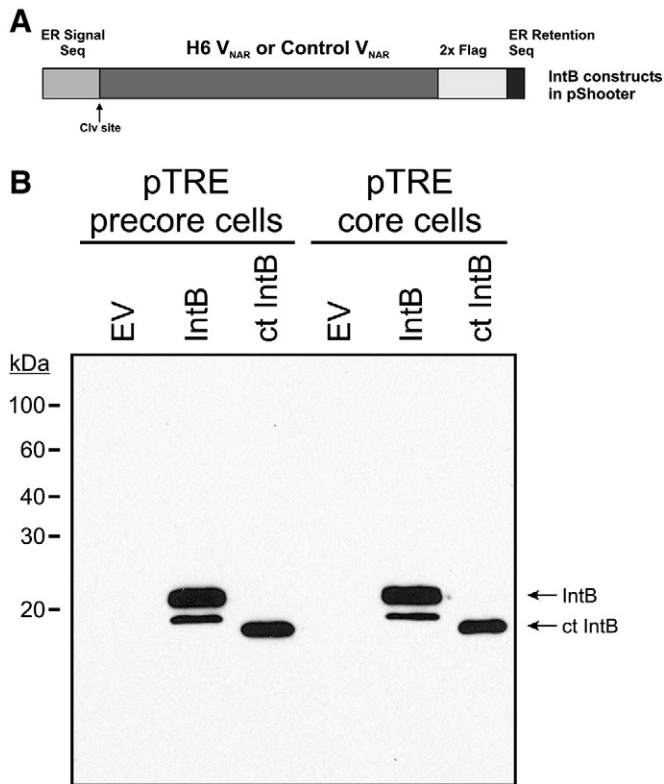


Fig. 4. Construction and expression of H6 Intrabody. (A) diagram illustrating the intrabody expression cassette in pShooter pCMV/ER vector. The H6 V_{NAR} or control V_{NAR} sequences with dual C-terminal FLAG tags were inserted into BssHII/XhoI restriction sites, in frame with an N-terminal ER signal sequence and a C-terminal ER retention sequence. (B) expression of H6 (IntB) and control intrabody (ct IntB) in comparison to empty vector (EV), transfected into Huh7 pTRE precore and core stable expression cell lines was confirmed by WB using anti-FLAG antibody detection. The H6 intrabody (IntB) displayed products with pre- and post-ER signal sequence cleavage.

Construction and validation of H6 intrabody

The precore precursor protein (p25) is localised to the ER via an ER signal sequence, and processed prior to export as the p17 HBeAg (Chen et al., 2008; Ito et al., 2009). To bind precore protein and inhibit secretion, H6 V_{NAR} intrabody expression was localised to the ER by cloning into the pCMV/ER plasmid, which incorporated an N-terminal ER signal sequence (cleaved upon ER localisation) and a C-terminal ER retention motif to prohibit intrabody and bound target protein secretion (Fig. 4A). Western Blotting (WB) analysis of precore- and core-expressing pTRE cell lines transfected with intrabody (IntB), control intrabody (ct IntB) or empty vector (EV), demonstrated effective intrabody expression (Fig. 4B). The H6 intrabody was detected in both cell lines as a doublet band, representing pre- and post-ER signal sequence cleavage. The ct IntB was not as effectively processed for signal sequence removal.

Intrabody effect on HBV precore protein *in vitro*

To investigate the intrabody effect on precore protein, the intrabody (IntB) construct (and control intrabody, ct IntB; and empty vector, EV) was transfected into precore, core and control pTRE cell lines, which stably express the specified HBV (genotype D) proteins, and also into AD38 and HepG2.2.15 HBV-expressing (genotype D) cell lines. Cell lysates (lys) and supernatants (sn) were analysed by WB (Fig. 5) and quantitative HBeAg Architect assay (Fig. 6). WB data and subsequent densitometry analysis (Fig. 5) suggested intrabody (IntB) treatment regulated precore/HBeAg (p25 and p17) in comparison to control intrabody (ct IntB) and empty

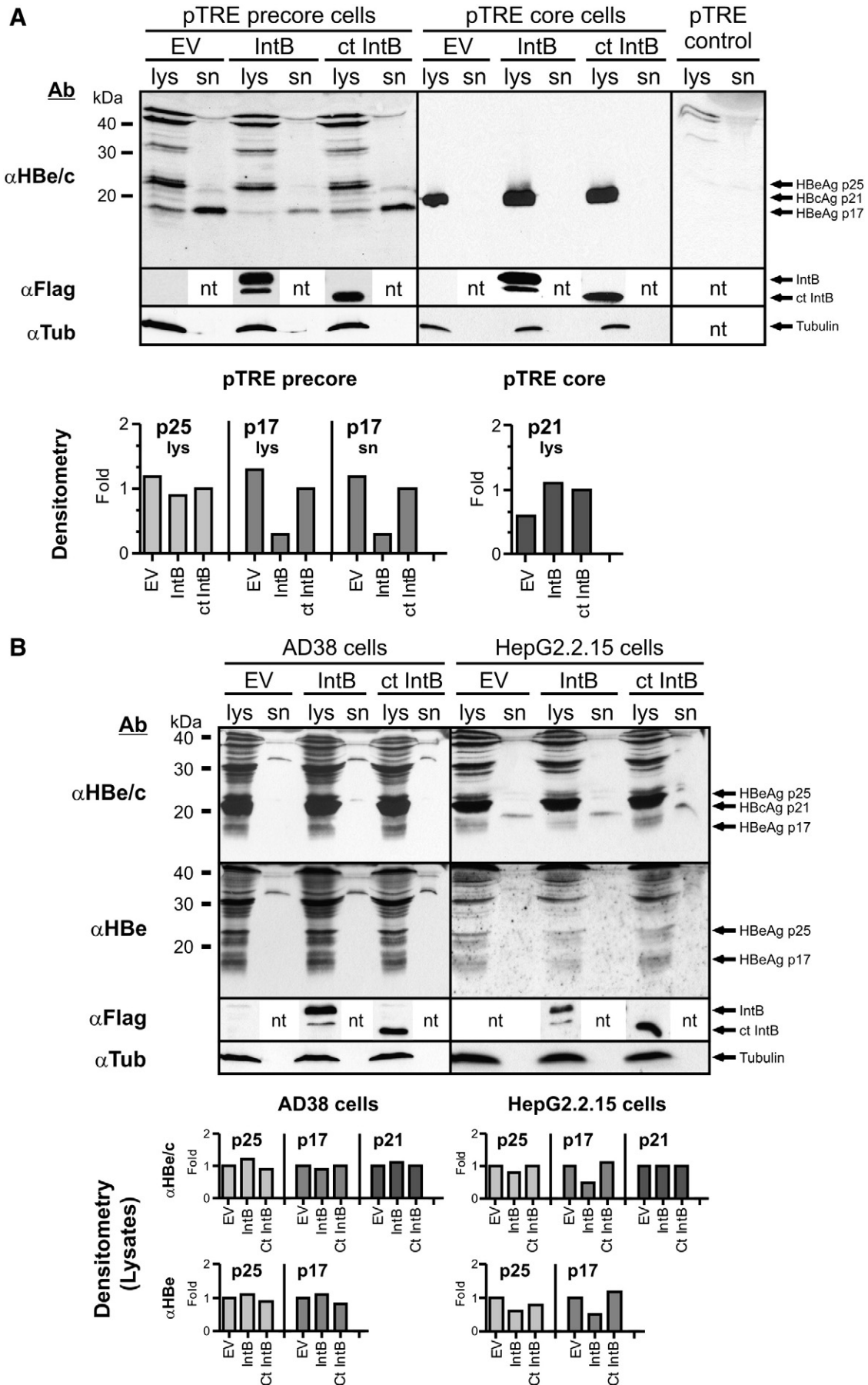
vector (EV) controls. Intrabody (IntB) treatment of pTRE precore cells (Fig. 5A) demonstrated a decrease in intracellular p25 levels (0.9 fold), possibly indicating an increase in ER degradation, coupled with a dramatic reduction of secreted p17 HBeAg (0.3 fold). These data strongly suggested that the intrabody is capable of disrupting precore processing and reducing p17 secretion. The core protein (p21) was unaffected by intrabody treatment, either due to a failure of intrabody to recognise p21 core *in vitro* (suggested in Fig. 2E), or due to a differential subcellular localisation of intrabody in the ER, and the p21 core localised to the cytosol. The AD38 cells (Fig. 5B), which are HBeAg secretion incompetent and virion secretion impaired, displayed a very minor (1.1–1.2 fold) increase of intracellular p25 with intrabody treatment, and no significant effect on intracellular p17 levels (0.9–1.1 fold). The intrabody transfected HepG2.2.15 cells (Fig. 5B), which exhibit partially impaired secretion, showed both reduced intracellular p25 (0.6–0.8 fold) and significantly reduced secreted p17 HBeAg (0.5 fold), similar to the response observed in pTRE precore cells. This further supported precore/HBeAg regulation and reduced secretion with *in vitro* intrabody treatment.

Analysis of intrabody treatment of the pTRE precore and core, and the AD38 cell lines by quantitative HBeAg Architect assay (Fig. 6) supported the WB data. Intrabody (IntB) treatment had no recognisable effect on p21 core protein (Fig. 6B), as expected, however p17 was reduced in pTRE precore (Fig. 6A) supernatant (0.7 fold) similar to the WB response. In the secretion incompetent AD38 cell lysates (Fig. 6C) p25/p17 increased (1.4 fold), which was suggestive of ER accumulation and interference with precore processing.

The effects of intrabody treatment on pTRE cell lines (precure, core and control) were examined using triple label immunostaining for confocal microscopy (Fig. 7). Cells were antibody stained for anti-HBe/c (magenta) expression, intrabody (green) expression (FLAG tag), and the ER (red) subcellular compartment (PDI), in order to investigate co-localisation and intrabody effect on precore protein. Overlay of the anti-HBe and IntB staining indicated co-localisation (white area) of the intrabody and precore protein (pTRE precure cells). Furthermore, triple staining overlays indicated localisation to the ER (white area). Co-localisation was not observed in pTRE core or control cells, or with control intrabody transfection. Most interesting was that precure protein staining appeared to be modified when co-localised in the cells with transfected anti-HBe intrabody. Staining patterns changed from punctate to ubiquitous in appearance (Fig. 7, pTRE precure cells), possibly suggesting intrabody treatment inhibited some level of intracellular precure aggregation. This modification to intracellular precure protein could translate into increased ER degradation to reduce p17 HBeAg secretion. Decreased precure aggregation may also improve p25 detection by WB and architect assay techniques, through allowing improved epitope accessibility for detection.

Discussion

This study describes the characterisation and *in vitro* intrabody application of an isolated V_{NAR} single domain antibody targeting the HBeAg of HBV. Screening of an *in vitro* naïve bacteriophage-displayed library of V_{NAR} domains, containing both synthetic and natural CDR3 loops, against the HBeAg target protein, isolated two V_{NAR} s designated H6 and H3. This selection process mirrors the antigen-driven selection/proliferation/maturation process seen in the natural shark immune system. Perhaps not surprisingly, given the close homology (149 common residues) between HBeAg and HBcAg, which are transcribed from a shared ORF, there was low level cross-reactivity by both V_{NAR} s to recombinant HBcAg (truncated), although HBeAg was dominantly recognised. There was, however, no affinity displayed for *in vitro* p21 core, which is likely due to additional protein processing/folding in eukaryotic cells. Although it is uncertain how structurally related these two HBV proteins are, the cross-reactivity observed here varied by approximately 2-fold affinity, which is indicative of minor



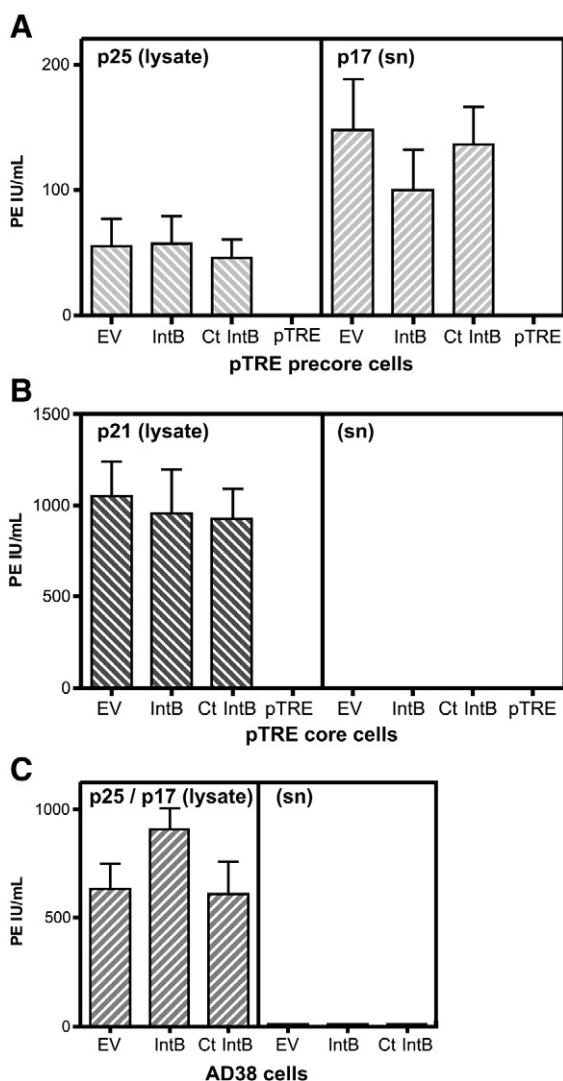


Fig. 6. Quantitative Architect assay analysis (PE IU/mL) of precore (p25 and p17) and core (p21) antigen levels in cell lysates and supernatants following *in vitro* intrabody transfection. (A) Huh7 pTRE precore cells transfected with H6 intrabody (IntB) versus control intrabody (ct IntB) and empty vector (EV), or non-expressing control pTRE cells. (B) as for (A) except using Huh7 pTRE core cells. (C) as for (A) except using AD38 HBV infectious cells, which are secretion incompetent.

variations in protein conformation subtly altering the antibody-binding site. The isolated V_{NARS} , H6 and H3, shared close homology, differing at only 4 residues (one in the CDR1 loop), but were significantly different from other V_{NARS} selected from this library in both their framework and CDR sequences, with a long CDR3 loop (18 residues) biased toward bulky hydrophobic residues. Despite differing at only 4 residues, H6 had a 2-fold increase in binding affinity compared with H3 for HBeAg. The difference between the two V_{NARS} relates to their sequence variation, which occurred most significantly in the CDR1 loop (Ser³³/Gly³³) but also in the top of heavy loop 4 (residues Asn⁶⁰/Ser⁶⁰ and Thr⁶²/Gly⁶²), a region increasingly recognised as important in the V_{NAR} -antigen interaction (Dooley et al., 2006; Kopsidas et al., 2006). Based on superior recognition of the target antigen, V_{NAR} H6 was selected for further investigation. Validation of

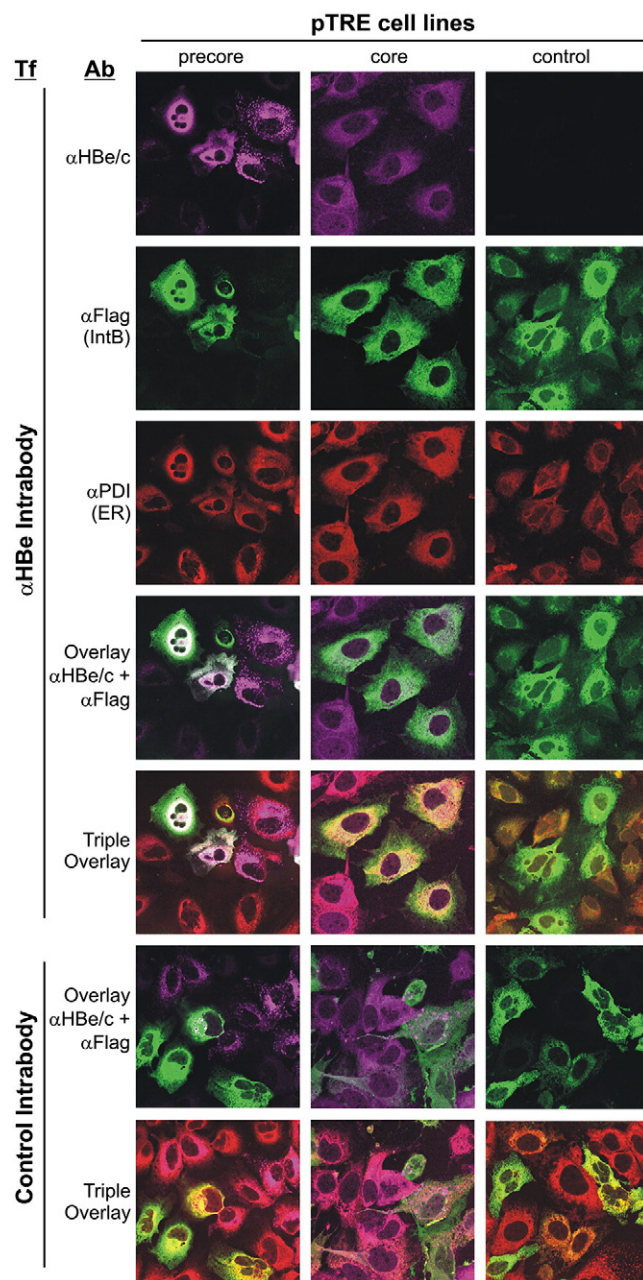


Fig. 7. Confocal immunostaining analysis of Huh7 pTRE precore, core and control cell lines transfected (Tf) with anti-HBe intrabody versus control intrabody. Transfected cells were triple stained with 1D8 anti-HBe/c conjugated to AlexaFluor647 (magenta), anti-FLAG FITC (green) for intrabody, and rabbit anti-PDI with anti-rabbit Texas Red secondary (red) for ER localisation. Overlays of double and triple staining display regions of co-localisation (white).

the H6 V_{NAR} determined a high degree of affinity and specificity for recombinant HBeAg (overall K_D of 53 nM) and HbcAg (90 nM), which is comparable with affinities reported for camelid $V_{\text{H}}\text{H}$ domains (Muyldermans and Lauwereys, 1999) and for scFv and disulphide stabilised Fv fragments (Reiter et al., 1996). The affinity of the V_{NAR} H6 for HBeAg and HbcAg exhibited a rapid association rate, a feature of V_{NAR} antibodies (SN, unpublished data). This may be due to the rigidity

Fig. 5. Analysis of intrabody effect on HBeAg expression *in vitro*. WB analysis (upper) of HBeAg regulation in Huh7 pTRE precore, core or control stable cell lines (A), or AD38 and HepG2.2.15 HBV-expressing cell lines (B), transfected with H6 intrabody (IntB), control intrabody (ct IntB) or empty vector (EV). Cells were harvested for cell lysate (lys) and extracellular supernatant (sn). Blots were probed with anti-HBe/c, anti-HBe (AD38 and HepG2.2.15 only to discriminate between p25/17 and p21), anti-FLAG for intrabody expression, and also with anti-Tubulin (Tub) for total cell lysate loading control. Densitometry (lower) was performed on the detected precore/HBeAg (p25 and p17) and core (p21) proteins in lys and sn (pTRE cell lines only as AD38 and HepG2.2.15 cell lines secretion compromised), which was reported as fold change. *nt* designates not tested.

imparted by a CDR1–CDR3 disulphide bridge allowing rapid association, followed by adoption of an induced fit type configuration (Stanfield et al., 2007) contributing to high affinity binding.

The ability of the V_{NAR} extended CDR3 loop to bind cryptic antigen pockets suggests a conformational recognition epitope. Many conventional anti-HBe/HBc (cross-reactive) antibodies target a common linear epitope, the immunodominant loop (residues 74–83) located at the α -helical spike of dimerised capsid subunit (Steven et al., 2005). We hypothesised that the V_{NAR} H6 domain recognises an alternative conformational target site of HBeAg/HBcAg, by virtue of the extended CDR3 loop. Peptide ELISA analysis using HBeAg linear epitopes supported this, with specific H6 V_{NAR} affinity absent. Resolution of the H6 V_{NAR} target epitope may depend on the co-crystal structure determination of the HBeAg/H6 V_{NAR} and/or HBcAg/H6 V_{NAR} binding complexes. Structural determination of the V_{NAR} binding site would further allow for structure based design of the V_{NAR} to improve binding affinity.

We further developed the H6 V_{NAR} as an intrabody with intracellular ER localised delivery to target intracellular precore protein, and an ER retention signal to interfere with bound HBeAg secretion, thus reducing extracellular HBeAg load. Intrabody transfection of precore- or core-expressing pTRE cell lines (genotype D), or HBV-expressing (genotype D) cell line (HepG2.2.15), showed a common trend for a considerable downregulation of secreted p17 HBeAg, and downregulation of p25 intracellular precore, the scale of which was cell line dependant, potentially due to cell line background differences. Importantly, despite significant sequence homology and cross-reactivity to recombinant HBcAg (truncated), there was no intrabody regulation of p21 core *in vitro*. This was likely due to different structural folding/epitope display between precore and core protein *in vitro*, or due to limited ER localised intrabody access to the cytoplasmic core antigen. In addition, the intrabody interfered with intracellular precore processing/folding. *In vitro* transfection and co-localisation of intrabody and precore to the ER, which was demonstrated with confocal immunostaining analysis, altered precore staining from the typical punctate/aggregated state to a ubiquitous appearance. This suggests intrabody inhibits precore aggregation or promotes ER degradation/processing of precore to circumvent aggregation, and indicates that an anti-HBe V_{NAR} may possess therapeutic potential.

Immunoglobulins play an integral role in mediating and modulating the immune system, and research interests have increased to develop immunoglobulins as novel therapeutics and diagnostics (Nuttall and Walsh, 2008). The V_{NAR} capabilities make them suitable as protein reagents for diagnostic biosensor or proteomics applications, and furthermore, for development as immunoglobulin therapies (Wesolowski et al., 2009). Indeed, there is precedence for the treatment of HBV by immunoglobulin therapy (HBIg) (Schilling et al., 2003), and more specifically, downregulation of the innate response (TNF production) by HBeAg has been shown to be blocked *in vitro* by treatment with anti-HBe polyclonal antibody (Visvanathan et al., 2007). Engineering immunoglobulin domains (including V_{NAR} 's) as intrabodies may offer several therapeutic applications through inhibiting target protein interactions or function, promoting degradation or cell death, or disruption of subcellular localisation. Therapies under development target: tumour antigens; infectious diseases (e.g. HIV Tat protein [Bai et al., 2003] or HBV surface and core antigens [Serruys et al., 2009, 2010]); transplantation; protein mutation-associated diseases (e.g. prion proteins [Cardinale et al., 2005]); and, protein aggregation diseases (Alzheimer's [Lynch et al., 2008]). To circumvent present intrabody therapy issues related to *in vivo* gene delivery, the intrabody *in vitro* validated anti-HBe V_{NAR} , could be engineered as a humanized antibody for *in vivo* immunoglobulin therapy.

In this study we have utilised a V_{NAR} molecular library targeting the HBeAg of HBV at mid-nanomolar range affinities. V_{NAR} molecules offer distinct advantages of compact size, robust stability and cryptic

antigenic epitope access via unusually long and variable CDR3 loops (Nuttall et al., 2004; Stanfield et al., 2004; Streltsov et al., 2004, 2005). Overall, this study presents an isolated V_{NAR} domain targeting HBeAg which has been further developed for intrabody activity *in vitro* to establish effective regulation of intracellular precore, alteration of precore processing/folding intracellularly, and reduction of extracellular HBeAg. Regulation of extracellular HBeAg is a valuable therapeutic tool to improve treatment efficacy, and avoid CHB progression. HBeAg titres above ~200 PE IU/mL result in higher treatment failure rates, with response to IFN treatment enhanced with lower HBeAg titres (Fried et al., 2008). Treatment to reduce HBeAg load prior to IFN- α therapy has potential to improve patient IFN treatment outcome. Further research to develop this treatment for *in vivo* study, such as engineering human Fc domains to create chimeric antibodies for delivery, would be an important step in assessing future therapeutic potential and the promotion of antiviral effectiveness.

Materials and methods

Recombinant HBeAg protein expression and purification

Full-length HBeAg and C-terminally truncated HBcAg (149 residues) from HBV genotype D (Delaney and Isom, 1998) were cloned into pGEX-6-1 vector (GE Healthcare, Uppsala, Sweden), and protein expressed in BL21(DE3) *Escherichia coli* (*E. coli*) cells (Novagen, Madison, WI, USA). Soluble recombinant protein was purified on glutathione Sepharose 4B beads (GE Healthcare). Fusion proteins were either competitively eluted from the glutathione Sepharose with 10 mM reduced glutathione (Roche, Indianapolis, IN, USA), or were cleaved from the GST fusion tag (on the resin) using PreScission protease (GE Healthcare). Purified recombinant protein was dialysed into PBS or 10–50 mM Tris pH 7.0–7.5, concentrated and quality assessed by SDS-PAGE, SEC and N-terminal protein sequencing.

V_{NAR} library selection and protein expression

Construction of the Wobbegong (*Orectolobus maculatus*) V_{NAR} library (~ 4.0×10^8 independent clones) has been described previously (Nuttall et al., 2003). Phagemid particles carrying the V_{NAR} -gene3 protein were propagated and isolated by standard procedures (Galanis et al., 1997). For biopanning of the phagemid library, recombinant HBeAg (1.25–3.75 $\mu\text{g}/\text{ml}$ in PBS) was coated on to Maxisorb Immunotubes at 4 °C overnight, and panning undertaken as described previously (Nuttall et al., 2003). Phagemid particles were eluted using 2% triethylamine and neutralised by the addition of 1 M Tris pH 7.5. Four rounds of panning were performed, with the stringency of selection increasing at each round. Following final selection, *E. coli* TG1 were infected with phagemid particles and plasmids propagated. The V_{NAR} cassette was extracted as a *NotI/SfiI* fragment and subcloned into pGC cloning/expression vector (Coia et al., 1997), and clones sequenced (GenBank database accession numbers EU213060 and EU213061) using BigDye terminator sequencing kit (Applied Biosystems, USA). Recombinant V_{NAR} protein was expressed in *E. coli* as previously described (Nuttall et al., 2001), and periplasmic fractions isolated (Minsky et al., 1986) and either used as crude fractions, or recombinant protein purified using an anti-FLAG antibody-Sepharose column, and eluted with Immunopure® gentle elution buffer (GEB; Pierce, Rockford, IL, USA), dialysed into PBS or 10 mM Tris pH 7.0–7.5, and concentrated. Protein purity was analysed by SDS-PAGE and by SEC.

Biosensor binding analysis

SPR measurements were performed using a Biacore T100 biosensor system (Biacore AB, Uppsala, Sweden). CM5 sensor chips, mouse anti-GST IgG antibody (α -GST), and all buffers were sourced from GE

Healthcare. All experiments were performed at 25 °C in 1x HBS-EP + buffer (10 mM HEPES, 150 mM NaCl, 3 mM EDTA, 0.05% surfactant P-20, pH 7.4). An indirect binding assay was used to analyse the interaction between V_{NAR} analyte and HBeAg or HBcAg (Fig. 3A). A standard coupling protocol (Biacore T100 control software version 1.1) was employed to immobilise the α -GST antibody (30 $\mu\text{g}/\text{ml}$, 10 mM sodium acetate pH 5.0) at ~4000 response units (RU) (Johnsson et al., 1991) in flow cells 1 (reference surface) and 2 (test surface). HBeAg-GST or HBcAg-GST (20 $\mu\text{g}/\text{ml}$) were injected (30 $\mu\text{l}/\text{min}$) over α -GST surface resulting in a capture of approximately 264.5 ± 12.4 RU of recombinant protein. V_{NAR} preparations (26.25 to 420 nM), were injected (30 $\mu\text{l}/\text{min}$) serially over the α -GST/HBe/cAg-GST (Fig. 3A) and reference surfaces. Association and dissociation phases were each monitored for 10 min. The V_{NAR} and antigen surfaces were regenerated within the dissociation phase, and the HBeAg-GST or HBcAg-GST surfaces were regenerated between each set of V_{NAR} concentrations with 10 mM glycine pH 2.2. To determine the kinetic parameters of the interactions, each data set was double-referenced and fit globally to a 1:1 interaction model using Biacore T100 evaluation software (version 1.1).

Antibodies

The following primary antibodies were utilised: mouse anti-FLAG monoclonal antibody (mAb) (WEHI, Australia); mouse anti-HBe mAb (Fitzgerald, Concord, MA, USA); 1D8 mouse anti-HBe/c (VIDRL); 7E9 mouse anti-HBe (VIDRL); mouse anti-Tubulin (Abcam, Cambridge, UK); and rabbit anti-PDI (ER stain) (SantaCruz, Santa Cruz, CA, USA). The following horseradish peroxidase (HRP)-conjugated secondary antibodies were utilised: goat anti-mouse immunoglobulin (Ig) (Pierce); goat anti-rabbit HRP IgG H + L (Biorad, Hercules, CA, USA); rabbit anti-mouse IgG (Dako); and mouse anti-FLAG M2 IgG (Sigma, St Louis, USA). The following secondary antibodies were utilised in immunostaining: mouse anti-FLAG FITC conjugate (Sigma); and goat anti-rabbit Texas red conjugate (Abcam).

V_{NAR} characterisation ELISA

For ELISA assays, recombinant proteins (0.4 $\mu\text{g}/\text{well}$) in PBS were coated onto Maxisorb Immuno-plates (Nunc, Germany). Between each step plates were rinsed twice with PBS and once with PBS/0.05% Tween20. Wells were blocked with PBS/5% skim milk powder (Blotto) for 1 h, before incubation with V_{NAR} periplasmic fractions or recombinant protein for 1 h. Primary antibody in PBS/5% Blotto was added, followed by HRP conjugated secondary antibody (in PBS/5% Blotto). Plates were developed using ABTS (2,2 azino di-(ethyl) benzthiazoline sulphonic acid [Roche]), and absorbance read at $A_{405\text{nm}}$.

Cloning V_{NAR} into eukaryotic pCMV/ER expression vector

The H6 and control V_{NAR} sequences including a double C-terminal FLAG tag were PCR amplified with BssHIII (Roche) and XhoI (Roche) restriction sites. Digested insert was ligated into similarly cut pShooter pCMV/ER expression plasmid (Invitrogen, Carlsbad, CA, USA), in frame with an N-terminal ER signal sequence and a C-terminal ER retention sequence (Fig. 4A), the former of which is cleaved from the V_{NAR} protein upon ER localisation.

Cells and transfections

The following cells lines were used in intrabody transfection experiments: Tetracycline (Tet) responsive Huh7 pTRE genotype D precore (p25), core (p21) and control (empty vector) stable cell lines (Locarnini et al., 2005); AD38 (Tet responsive) and HepG2.2.15 cells, which express HBV genotype D (Ladner et al., 1997; Sells et al., 1987). Transfections of intrabody, control intrabody and empty vector were

performed as described below. pTRE cells lines (maintained Tet off for 7 days) were transfected with 2.2 μg DNA and 9.1 μl Fugene (Roche) per 60 mm dishes according to manufacturer' instructions. AD38 (maintained Tet off for 7 days) and HepG2.2.15 cells were transfected with 13.5 μg DNA and 21.6 μl Fugene per 100 mm dish. Transfection reactions were adjusted according to the surface area of the culture vessel. Precore & core protein for ELISA was produced from Huh7 cells (Nakabayashi et al., 1982) transfected with constructs of pCI precore (p25), pCI core (p21) and pCI empty vector using 3.8 μg DNA and 9.1 μl Fugene per 60 mm dish.

Analysis of precore/HBeAg in intrabody transfected cells

Transfected cells were harvested for protein analysis of extracellular supernatant (sn) and intracellular lysate (lys). Sn was pelleted at 3000 rpm 5 min 4 °C to remove cell debris. Cell lysates were harvested in 800 μl cell lysis buffer (50 mM Tris pH 7.5, 1 mM EDTA, 150 mM NaCl, 0.5% NP40) for 15 min at RT, and nuclear material removed by centrifugation at 16,000 \times g 5 min. Cell lys and sn were analysed by WB and quantitative HBeAg serological assay (Architect, Abbott, Chicago, IL, USA) (Thompson et al., 2010). For WB, samples were resolved on SDS-PAGE gels (12.5%) and transferred to nitrocellulose (GE Healthcare) according to standard protocols. Proteins were detected using the following antibodies: mouse 1D8 anti-HBe/c HRP; mouse 7E9 anti-HBe and mouse anti-FLAG HRP; and mouse anti-Tubulin and rabbit anti-mouse HRP. Blots were developed with chemiluminescence as per manufacturer's protocol (Perkin Elmer, Waltham, MA, USA), and stripped for reprobing as per manufacturer's protocol (Abcam). Cell lys and sn were also analysed by HBeAg serological assay (Architect), as per manufacturer's instructions, and were run against PE IU/mL standardised HBeAg samples for quantification.

Immunostaining of intrabody transfected cells

Coverslips of transfected pTRE precore, core and control cells were fixed in 4% paraformaldehyde (PFA) for 20 min and permeabilised in 0.5% TritonX-100 for 8 min. Coverslips were blocked in 1% BSA in PBS, and stained with the following primary and secondary antibodies in 1% BSA in PBS: mouse 1D8 anti-HBe/c Alexafluor647 conjugate; mouse anti-FLAG FITC conjugate; rabbit anti-PDI (ER stain); and goat anti-rabbit Texas red conjugate. Coverslips were mounted in FluoroPrep (BioMerieux, France), and analysed using a laser scanning spectral (Leica TCS SP2) confocal microscope (Leica Microsystems, Germany) using Leica confocal software.

Acknowledgments

We thank Ms Vanessa Hughes, Ms Julie Angerosa and Ms Meghan Hattaki for the technical assistance with this research. We thank Mr Nick Bartone for the oligonucleotide synthesis and Mr Phil Strike for the N-terminal protein sequencing. The Co-operative Research Centre for Diagnostics is acknowledged for their partial financial support of this work, as is the Bristol-Myers Squibb Freedom to discover award to Stephen Locarnini.

References

- Bai, J., Sui, J., Zhu, R.Y., Tallarico, A.S., Gennari, F., Zhang, D., Marasco, W.A., 2003. Inhibition of Tat-mediated transactivation and HIV-1 replication by human anti-hCyclinT1 intrabodies. *J. Biol. Chem.* 278 (3), 1433–1442.
- Cardinale, A., Filesi, I., Vetrugno, V., Pocchiari, M., Sy, M.S., Biocca, S., 2005. Trapping prion protein in the endoplasmic reticulum impairs PrPc maturation and prevents PrPsc accumulation. *J. Biol. Chem.* 280 (1), 685–694.
- Chang, C., Enders, G., Sprengel, R., Peters, N., Varmus, H.E., Ganem, D., 1987. Expression of the precore region of an avian hepatitis B virus is not required for viral replication. *J. Virol.* 61 (10), 3322–3325.

- Chen, R.Y., Edwards, R., Shaw, T., Colledge, D., Delaney, W.E.T., Isom, H., Bowden, S., Desmond, P., Locarnini, S.A., 2003. Effect of the G1896A precore mutation on drug sensitivity and replication yield of lamivudine-resistant HBV in vitro. *Hepatology* 37 (1), 27–35.
- Chen, M.T., Billaud, J.N., Sallberg, M., Guidotti, L.G., Chisari, F.V., Jones, J., Hughes, J., Milich, D.R., 2004. A function of the hepatitis B virus precore protein is to regulate the immune response to the core antigen. *Proc. Natl Acad. Sci. USA* 101 (41), 14913–14918.
- Chen, M., Sallberg, M., Hughes, J., Jones, J., Guidotti, L.G., Chisari, F.V., Billaud, J.N., Milich, D.R., 2005. Immune tolerance split between hepatitis B virus precore and core proteins. *J. Virol.* 79 (5), 3016–3027.
- Chen, C.Y., Crowther, C., Kew, M.C., Kramvis, A., 2008. A valine to phenylalanine mutation in the precore region of hepatitis B virus causes intracellular retention and impaired secretion of HBe-antigen. *Hepatology* 38 (6), 580–592.
- Chothia, C., Lesk, A.M., Tramontano, A., Levitt, M., Smith-Gill, S.J., Air, G., Sheriff, S., Padlan, E.A., Davies, D., Tulip, W.R., et al., 1989. Conformations of immunoglobulin hypervariable regions. *Nature* 342 (6252), 877–883.
- Coia, G., Ayres, A., Lilley, G.G., Hudson, P.J., Irving, R.A., 1997. Use of mutator cells as a means for increasing production levels of a recombinant antibody directed against Hepatitis B. *Gene* 201 (1–2), 203–209.
- Delaney, W.E.T., Isom, H.C., 1998. Hepatitis B virus replication in human HepG2 cells mediated by hepatitis B virus recombinant baculovirus. *Hepatology* 28 (4), 1134–1146.
- Dienes, H.P., Gerken, G., Goergen, B., Heermann, K., Gerlich, W., Meyer zum Buschenfelde, K.H., 1995. Analysis of the precore DNA sequence and detection of precore antigen in liver specimens from patients with anti-hepatitis B e-positive chronic hepatitis. *Hepatology* 21 (1), 1–7.
- Dooley, H., Flajnik, M.F., 2006. Antibody repertoire development in cartilaginous fish. *Dev. Comp. Immunol.* 30 (1–2), 43–56.
- Dooley, H., Stanfield, R.L., Brady, R.A., Flajnik, M.F., 2006. First molecular and biochemical analysis of in vivo affinity maturation in an ectothermic vertebrate. *Proc. Natl Acad. Sci. USA* 103 (6), 1846–1851.
- Fried, M.W., Piratvisuth, T., Lau, G.K., Marcellin, P., Chow, W.C., Cooksley, G., Luo, K.X., Paik, S.W., Liaw, Y.F., Button, P., Popescu, M., 2008. HBeAg and hepatitis B virus DNA as outcome predictors during therapy with peginterferon alfa-2a for HBeAg-positive chronic hepatitis B. *Hepatology* 47 (2), 428–434.
- Galanis, M., Irving, R.A., Hudson, P.J., 1997. Bacteriophage library construction and selection of recombinant antibodies. *Current protocols in Immunology*. John Wiley and Sons, NY, pp. 17.1.1–17.1.45.
- Greenberg, A.S., Avila, D., Hughes, M., Hughes, A., McKinney, E.C., Flajnik, M.F., 1995. A new antigen receptor gene family that undergoes rearrangement and extensive somatic diversification in sharks. *Nature* 374 (6518), 168–173.
- Ito, K., Kim, K.H., Lok, A.S., Tong, S., 2009. Characterization of genotype-specific carboxyl-terminal cleavage sites of hepatitis B virus e antigen precursor and identification of furin as the candidate enzyme. *J. Virol.* 83 (8), 3507–3517.
- Johnsson, B., Lofas, S., Lindquist, G., 1991. Immobilization of proteins to a carboxymethyl-dextran-modified gold surface for biospecific interaction analysis in surface plasmon resonance sensors. *Anal. Biochem.* 198 (2), 268–277.
- Kane, M.A., 1996. Global status of hepatitis B immunisation. *Lancet* 348 (9029), 696.
- Kopsidas, G., Roberts, A.S., Coia, G., Streltsov, V.A., Nuttall, S.D., 2006. In vitro improvement of a shark IgNAR antibody by Qbeta replicase mutation and ribosome display mimics in vivo affinity maturation. *Immunol. Lett.* 107 (2), 163–168.
- Ladner, S.K., Otto, M.J., Barker, C.S., Zaifert, K., Wang, G.H., Guo, J.T., Seeger, C., King, R.W., 1997. Inducible expression of human hepatitis B virus (HBV) in stably transfected hepatoblastoma cells: a novel system for screening potential inhibitors of HBV replication. *Antimicrob. Agents Chemother.* 41 (8), 1715–1720.
- Lavanchy, D., 2004. Hepatitis B virus epidemiology, disease burden, treatment, and current and emerging prevention and control measures. *J. Viral Hepat.* 11 (2), 97–107.
- Locarnini, S., Shaw, T., Dean, J., Colledge, D., Thompson, A., Li, K., Lemon, S.M., Lau, G.G., Beard, M.R., 2005. Cellular response to conditional expression of the hepatitis B virus precore and core proteins in cultured hepatoma (Huh-7) cells. *J. Clin. Virol.* 32 (2), 113–121.
- Lynch, S.M., Zhou, C., Messer, A., 2008. An scFv intrabody against the nonamyloid component of alpha-synuclein reduces intracellular aggregation and toxicity. *J. Mol. Biol.* 377 (1), 136–147.
- Messageot, F., Salhi, S., Eon, P., Rossignol, J.M., 2003. Proteolytic processing of the hepatitis B virus e antigen precursor. Cleavage at two furin consensus sequences. *J. Biol. Chem.* 278 (2), 891–895.
- Milich, D.R., Jones, J.E., Hughes, J.L., Price, J., Raney, A.K., McLachlan, A., 1990. Is a function of the secreted hepatitis B e antigen to induce immunologic tolerance in utero? *Proc. Natl Acad. Sci. USA* 87 (17), 6599–6603.
- Milich, D.R., Chen, M.K., Hughes, J.L., Jones, J.E., 1998. The secreted hepatitis B precore antigen can modulate the immune response to the nucleocapsid: a mechanism for persistence. *J. Immunol.* 160 (4), 2013–2021.
- Minsky, A., Summers, R.G., Knowles, J.R., 1986. Secretion of beta-lactamase into the periplasm of *Escherichia coli*: evidence for a distinct release step associated with a conformational change. *Proc. Natl Acad. Sci. USA* 83 (12), 4180–4184.
- Muyldermans, S., Lauwereys, M., 1999. Unique single-domain antigen binding fragments derived from naturally occurring camel heavy-chain antibodies. *J. Mol. Recognit.* 12 (2), 131–140.
- Nakabayashi, H., Taketa, K., Miyano, K., Yamane, T., Sato, J., 1982. Growth of human hepatoma cells lines with differentiated functions in chemically defined medium. *Cancer Res.* 42 (9), 3858–3863.
- Nuttall, S.D., Walsh, R.B., 2008. Display scaffolds: protein engineering for novel therapeutics. *Curr. Opin. Pharmacol.* 8 (5), 609–615.
- Nuttall, S.D., Krishnan, U.V., Hattarki, M., De Gori, R., Irving, R.A., Hudson, P.J., 2001. Isolation of the new antigen receptor from wobbegong sharks, and use as a scaffold for the display of protein loop libraries. *Mol. Immunol.* 38 (4), 313–326.
- Nuttall, S.D., Krishnan, U.V., Doughty, L., Pearson, K., Ryan, M.T., Hoogenraad, N.J., Hattarki, M., Carmichael, J.A., Irving, R.A., Hudson, P.J., 2003. Isolation and characterization of an IgNAR variable domain specific for the human mitochondrial translocase receptor Tom70. *Eur. J. Biochem.* 270 (17), 3543–3554.
- Nuttall, S.D., Humberstone, K.S., Krishnan, U.V., Carmichael, J.A., Doughty, L., Hattarki, M., Coley, A.M., Casey, J.L., Anders, R.F., Foley, M., Irving, R.A., Hudson, P.J., 2004. Selection and affinity maturation of IgNAR variable domains targeting *Plasmodium falciparum* AMA1. *Proteins* 55 (1), 187–197.
- Padlan, E.A., 1994. Anatomy of the antibody molecule. *Mol. Immunol.* 31 (3), 169–217.
- Reiter, Y., Brinkmann, U., Lee, B., Pastan, I., 1996. Engineering antibody Fv fragments for cancer detection and therapy: disulfide-stabilized Fv fragments. *Nat. Biotechnol.* 14 (10), 1239–1245.
- Revell, P., Yuen, L., Walsh, R., Perrault, M., Locarnini, S., Kramvis, A., 2010. Bioinformatic analysis of the hepadnavirus e-antigen and its precursor identifies remarkable sequence conservation in all orthohepadnaviruses. *J. Med. Virol.* 82, 104–115.
- Riordan, S.M., Skinner, N., Kurtovic, J., Locarnini, S., Visvanathan, K., 2006. Reduced expression of toll-like receptor 2 on peripheral monocytes in patients with chronic hepatitis B. *Clin. Vaccine Immunol.* 13 (8), 972–974.
- Roux, K.H., Greenberg, A.S., Greene, L., Strelets, L., Avila, D., McKinney, E.C., Flajnik, M.F., 1998. Structural analysis of the nurse shark (new) antigen receptor (NAR): molecular convergence of NAR and unusual mammalian immunoglobulins. *Proc. Natl Acad. Sci. USA* 95 (20), 11804–11809.
- Schilling, R., Ijaz, S., Davidoff, M., Lee, J.Y., Locarnini, S., Williams, R., Naoumov, N.V., 2003. Endocytosis of hepatitis B immune globulin into hepatocytes inhibits the secretion of hepatitis B virus surface antigen and virions. *J. Virol.* 77 (16), 8882–8892.
- Sells, M.A., Chen, M.L., Acs, G., 1987. Production of hepatitis B virus particles in Hep G2 cells transfected with cloned hepatitis B virus DNA. *Proc. Natl Acad. Sci. USA* 84 (4), 1005–1009.
- Serruys, B., Van Houtte, F., Verbrugge, P., Leroux-Roels, G., Vanlandschoot, P., 2009. Llama-derived single-domain intrabodies inhibit secretion of hepatitis B virions in mice. *Hepatology* 49 (1), 39–49.
- Serruys, B., Van Houtte, F., Farhoudi-Moghadam, A., Leroux-Roels, G., Vanlandschoot, P., 2010. Production, characterization and in vitro testing of HBcAg-specific VHH intrabodies. *J. Gen. Virol.* 91 (Pt 3), 643–652.
- Stanfield, R.L., Dooley, H., Flajnik, M.F., Wilson, I.A., 2004. Crystal structure of a shark single-domain antibody V region in complex with lysozyme. *Structure* 305 (5691), 1770–1773.
- Stanfield, R.L., Dooley, H., Verdino, P., Flajnik, M.F., Wilson, I.A., 2007. Maturation of shark single-domain (IgNAR) antibodies: evidence for induced-fit binding. *J. Mol. Biol.* 367 (2), 358–372.
- Steven, A.C., Conway, J.F., Cheng, N., Watts, N.R., Belnap, D.M., Harris, A., Stahl, S.J., Wingfield, P.T., 2005. Structure, assembly, and antigenicity of hepatitis B virus capsid proteins. *Adv. Virus Res.* 64, 125–164.
- Streltsov, V.A., Varghese, J.N., Carmichael, J.A., Irving, R.A., Hudson, P.J., Nuttall, S.D., 2004. Structural evidence for evolution of shark Ig new antigen receptor variable domain antibodies from a cell-surface receptor. *Proc. Natl Acad. Sci. USA* 101 (34), 12444–12449.
- Streltsov, V.A., Carmichael, J.A., Nuttall, S.D., 2005. Structure of a shark IgNAR antibody variable domain and modeling of an early-developmental isotype. *Protein Sci.* 14 (11), 2901–2909.
- Takahashi, K., Machida, A., Funatsu, G., Nomura, M., Usuda, S., Aoyagi, S., Tachibana, K., Miyamoto, H., Imai, M., Nakamura, T., Miyakawa, Y., Mayumi, M., 1983. Immunochemical structure of hepatitis B e antigen in the serum. *J. Immunol.* 130 (6), 2903–2907.
- Thompson, A.J., Nguyen, T., Iser, D., Ayres, A., Jackson, K., Littlejohn, M., Slavin, J., Bowden, S., Gane, E.J., Abbott, W., Lau, G.K., Lewin, S.R., Visvanathan, K., Desmond, P., Locarnini, S.A., 2010. Serum hepatitis B surface antigen and hepatitis B e antigen titers: disease phase influences correlation with viral load and intrahepatic hepatitis B virus markers. *Hepatology* 51 (6), 1933–1944.
- Visvanathan, K., Skinner, N.A., Thompson, A.J., Riordan, S., Sozzi, V., Edwards, R., Rodgers, S., Kurtovic, J., Chang, J., Lewin, S., Desmond, P., Locarnini, S., 2007. Regulation of Toll-like receptor-2 expression in chronic hepatitis B by the precore protein. *Hepatology* 45 (1), 102–110.
- Wesolowski, J., Alzogaray, V., Reyelt, J., Unger, M., Juarez, K., Urrutia, M., Cauerhff, A., Danquah, W., Rissiek, B., Scheuplein, F., Schwarz, N., Adriouch, S., Boyer, O., Seman, M., Licea, A., Serreze, D.V., Goldbaum, F.A., Haag, F., Koch-Nolte, F., 2009. Single domain antibodies: promising experimental and therapeutic tools in infection and immunity. *Med. Microbiol. Immunol.* 198 (3), 157–174.